

Deletion of *Gpr128* results in weight loss and increased intestinal contraction frequency

Ying-Yin Ni, Yan Chen, Shun-Yuan Lu, Bi-Ying Sun, Fang Wang, Xiao-Lin Wu, Su-Ying Dang, Guo-Hua Zhang, Hong-Xin Zhang, Yin Kuang, Jian Fei, Ming-Min Gu, Wei-Fang Rong, Zhu-Gang Wang

Ying-Yin Ni, Yan Chen, Fang Wang, Xiao-Lin Wu, Su-Ying Dang, Ming-Min Gu, Zhu-Gang Wang, Department of Medical Genetics, E-Institutes of Shanghai Universities, Shanghai Jiao Tong University School of Medicine, Shanghai 200025, China
Shun-Yuan Lu, Hong-Xin Zhang, Zhu-Gang Wang, Research Centre for Experimental Medicine, Rui Jin Hospital Affiliated with Shanghai Jiao Tong University School of Medicine, Shanghai 200025, China

Bi-Ying Sun, Guo-Hua Zhang, Wei-Fang Rong, Department of Physiology, Shanghai Jiao Tong University School of Medicine, Shanghai 200025, China

Yin Kuang, Jian Fei, Zhu-Gang Wang, Shanghai Research Centre for Model Organisms, Shanghai 201210, China

Author contributions: Rong WF and Wang ZG designed the research; Ni YY, Chen Y, Lu SY, Sun BY and Kuang Y performed the research; Wang F, Wu XL, Dang SY, Zhang GH and Zhang HX contributed new reagents/materials/analytic tools; Fei J, Gu MM, Rong WF and Wang ZG analyzed the data; Ni YY, Rong WF and Wang ZG wrote the paper.

Supported by Shanghai Municipal Health Bureau Foundation, No. 2010037; and the National Natural Science Foundation of China, Nos. 30900156, 81071444 and 31000986

Correspondence to: Wei-Fang Rong, Professor, Director, Department of Physiology, Shanghai Jiaotong University School of Medicine, 280 South Chongqing Road, Shanghai 200025, China. weifangrong@shsmu.edu.cn

Telephone: +86-21-63846590 Fax: +86-21-64370045

Received: June 14, 2013 Revised: September 15, 2013

Accepted: October 17, 2013

Published online: January 14, 2014

Abstract

AIM: To generate a *Gpr128* gene knockout mouse model and to investigate its phenotypes and the biological function of the *Gpr128* gene.

METHODS: Bacterial artificial chromosome-retrieval methods were used for constructing the targeting vector. Using homologous recombination and microinjection technology, a *Gpr128* knockout mouse model on a

mixed 129/BL6 background was generated. The mice were genotyped by polymerase chain reaction (PCR) analysis of tail DNA and fed a standard laboratory chow diet. Animals of both sexes were used, and the phenotypes were assessed by histological, biochemical, molecular and physiological analyses. Semi-quantitative reverse transcription-PCR and Northern blotting were used to determine the tissue distribution of *Gpr128* mRNA. Beginning at the age of 4 wk, body weights were recorded every 4 wk. Food, feces, blood and organ samples were collected to analyze food consumption, fecal quantity, organ weight and constituents of the blood and plasma. A Trendelenburg preparation was utilized to examine intestinal motility in wild-type (WT) and *Gpr128*^{-/-} mice at the age of 8 and 32 wk.

RESULTS: *Gpr128* mRNA was highly and exclusively detected in the intestinal tissues. Targeted deletion of *Gpr128* in adult mice resulted in reduced body weight gain, and mutant mice exhibited an increased frequency of peristaltic contraction and slow wave potential of the small intestine. The *Gpr128*^{+/+} mice gained more weight on average than the *Gpr128*^{-/-} mice since 24 wk, being 30.81 ± 2.84 g and 25.74 ± 4.50 g, respectively ($n = 10$, $P < 0.01$). The frequency of small intestinal peristaltic contraction was increased in *Gpr128*^{-/-} mice. At the age of 8 wk, the frequency of peristalsis with an intraluminal pressure of 3 cmH₂O was 6.6 ± 2.3 peristalsis/15 min in *Gpr128*^{-/-} intestine ($n = 5$) vs 2.6 ± 1.7 peristalsis/15 min in WT intestine ($n = 5$, $P < 0.05$). At the age of 32 wk, the frequency of peristaltic contraction with an intraluminal pressure of 2 and 3 cmH₂O was 4.6 ± 2.3 and 3.1 ± 0.8 peristalsis/15 min in WT mice ($n = 8$), whereas in *Gpr128*^{-/-} mice ($n = 8$) the frequency of contraction was 8.3 ± 3.0 and 7.4 ± 3.1 peristalsis/15 min, respectively (2 cmH₂O: $P < 0.05$ vs WT; 3 cmH₂O: $P < 0.01$ vs WT). The frequency of slow wave potential in *Gpr128*^{-/-} intestine (35.8 ± 4.3, 36.4 ± 4.2 and 37.1 ± 4.8/min with an intraluminal pressure of 1, 2 and 3 cmH₂O, $n = 8$) was also higher than in

WT intestine (30.6 ± 4.2 , 31.4 ± 3.9 and 31.9 ± 4.5 /min, $n = 8$, $P < 0.05$).

CONCLUSION: We have generated a mouse model with a targeted deletion of *Gpr128* and found reduced body weight and increased intestinal contraction frequency in this animal model.

© 2014 Baishideng Publishing Group Co., Limited. All rights reserved.

Key words: G-protein-coupled receptors; *Gpr128*; Knockout mouse; Weight loss; Intestinal contraction frequency

Core tip: The Adhesion family is the second largest subfamily of the G-protein-coupled receptors (GPCR). The physiological function of the orphan Adhesion-GPCR *Gpr128* is unknown. In the present study, we generated *Gpr128* knockout mice and confirmed the selective expression of *Gpr128* in the intestinal tissues. Phenotypic analysis revealed that targeted deletion of *Gpr128* in the mouse resulted in reduced body weight gain and increased frequency of peristaltic contraction and slow wave potential in the small intestine. The physiological roles of *Gpr128* in the gastrointestinal tract and its potential as a therapeutic target for obesity and nutritional disorders warrant further investigation.

Ni YY, Chen Y, Lu SY, Sun BY, Wang F, Wu XL, Dang SY, Zhang GH, Zhang HX, Kuang Y, Fei J, Gu MM, Rong WF, Wang ZG. Deletion of *Gpr128* results in weight loss and increased intestinal contraction frequency. *World J Gastroenterol* 2014; 20(2): 498-508 Available from: URL: <http://www.wjg-net.com/1007-9327/full/v20/i2/498.htm> DOI: <http://dx.doi.org/10.3748/wjg.v20.i2.498>

INTRODUCTION

G protein-coupled receptors (GPCRs) constitute one of the largest protein families in humans^[1,2] and play important roles in the transduction of intercellular signals across the plasma membrane *via* different G-proteins^[3,4]. GPCRs respond to a large variety of extracellular signals including small molecules such as Ca^{2+} , hormones, peptides, chemokines and other factors as well as sensory stimuli such as vision, smell, taste and neuronal transmission in response to photons^[5]. Due to their extremely diverse roles in biological processes, GPCRs represent important molecular targets for biomedical research and drug discovery^[6].

The adhesion family of GPCRs (Adhesion-GPCRs) is the second largest subfamily of GPCRs, with over 30 members found in mammals^[7,8]. These proteins are characterized by the dual presence of a secretin-like seven-transmembrane (7TM) domain and a long cell adhesion-like N-terminal domain, which typically consists of a

functional GPCR proteolytic site domain (GPS domain) and one or more conserved domains^[9,10]. Generally, the long N-termini bind various proteins that promote cell-to-cell and cell-to-matrix interactions^[11]. However, some Adhesion-GPCRs were found to have a GPS domain but to lack the conserved domains. *HE6* and *GPR56* are two such members for which no N-terminal conserved domains have been identified, although they have both been shown to have adhesive properties. *HE6* attachment appeared to be required for the maturation of germ cells because mutation of this receptor resulted in male infertility in mice^[12]. Mutations in *GPR56* have been shown to be associated with cortical malformation of the human brain^[13,14] and to participate in tumor cell adhesion^[15,16].

GPR128 is an orphan receptor of the Adhesion-GPCR family uncovered during BLASTP searches of the Celera database in 2003. *GPR128* is phylogenetically related to *HE6* and *GPR56* and lacks the conserved N-terminal domains apart from the GPS domain^[17]. The mouse *Gpr128* shares 69.9% homology with human *GPR128* and contains 16 exons.

GPCRs are expressed in virtually all tissue types in the body^[18]. However, some GPCRs are expressed in specific tissues and therefore are important targets for drug discovery^[19]. The tissue distribution of *GPR128*, as derived from the EST data or analysed by real-time quantitative polymerase chain reaction (RT-qPCR), shows specific patterns in human and mouse gastrointestinal tissue^[20,21]. However, until the commencement of this study, there was little information regarding the ligand or the physiological function of *GPR128* in mammals. Using PCR, Northern blotting and immunofluorescence staining, we show that *Gpr128* might be exclusively expressed in mouse intestine tissue. To study the role of *Gpr128* in the intestine, we generated mice with a targeted deletion of *Gpr128*. We found that *Gpr128* knockout mice exhibited less body weight gain and an increase in intestinal contraction frequency compared with their wild-type (WT) counterparts.

MATERIALS AND METHODS

Construction of the *Gpr128* targeting vector and electroporation of embryonic stem cells

The 129/Sv bacterial artificial chromosome (BAC) clone bMQ-239c21 was provided by the Sanger Institute. BAC-retrieval methods were used for constructing the targeting vector^[22,23].

The sequence, including the GPS domain and a portion of the 7TM domain, was retrieved from the BAC clone using a retrieval vector containing two homologous arms.

A targeting vector was constructed by replacing the mouse *Gpr128* genomic fragment (8.4 kb) covering exons 10-12 with the 1.9-kb phosphoglycerate kinase-neomycin resistance (PGK-Neo) cassette for positive selection and was laid with an external herpes simplex virus-1-thymi-

dine kinase cassette for negative selection^[24]. Additionally, this deletion causes an out-of-frame reading frame shift and thereby generates a loss-of-function allele.

The targeting vector contained 7.1 kb of homologous DNA upstream of the PGK-Neo cassette and 5.3 kb of homologous DNA downstream of the cassette as homologous recombination arms. After linearization, the targeting vector was electroporated into embryonic stem (ES) cells derived from 129/Sv G418- and GANC-resistant clones were selected using two pairs of PCR primers. The sequences of the primers used for identifying the recombinant clones are as follows: 5'-CCATAG-GAAGAATAATATCAACCAATC-3' (forward primer P1), 5'-CTGAGCCCAGAAAGCGAAGGA-3' (reverse primer P2), 5'-ACAAAAGCAAAACAAGGTCTG-GAAAG-3' (forward primer P3) and 5'-CCTCCCCCGT GCCTTCCCTTGAC-3' (reverse primer P4).

Generation of Gpr128 knockout mice

Chimeric male mice were generated by injecting the recombinant ES cell clone into C57BL/6 blastocysts, which were subsequently implanted into pseudopregnant female recipient mice. Germ line transmission was monitored by a coat color marker. Heterozygous mice were generated by crossing chimeras with WT 129/Sv female mice and selected for sib mating to create WT (*Gpr128*^{+/+}), heterozygous (*Gpr128*^{+/-}) and homozygous mice (*Gpr128*^{-/-}) for further experiments.

The mice were genotyped by PCR analysis of tail DNA using two primer pairs, which allows the amplification of WT and targeted alleles. The forward primer P3 and reverse primer P4 were used to amplify the 3' targeted allele, which yields a 5.7 kb band. The sequences of the primers used to amplify the WT allele are as follows: 5'-TCITCATCTCATTAGTTGGATGGGGTA-3' (forward primer P5) and 5'-ACAAAAGCAAAA-CAAGGTCTGGAAAG-3' (reverse primer P6). The length of the WT allele is 5.4 kb.

Semi-quantitative RT-PCR

All experiments involving animals were conducted under protocols approved by Institutional Animal Care and Use Committee of Shanghai Research Center for Model Organisms (Approval ID: 2010-0017), and the care of animals was in accord with the institution's guidelines.

The mice were anesthetized with ketamine and xylazine diluted in 0.9% saline, and all efforts were made to minimize animal suffering. Total RNA was extracted from adult mouse tissues using Trizol reagent (Invitrogen, Carlsbad, CA, United States) according to the manufacturer's instructions. For RT-PCR analysis, total RNA was treated with RNase-free DNase I (Promega, Fitchburg, Wisconsin, United States) and quantitated. A 1- μ g sample of total RNA was reverse-transcribed to cDNA with an RNA PCR kit (Takara, Dalian, Liaoning, China) according to the standard protocol. A fragment of *Gpr128* was amplified (25 cycles) with forward primer R1 (5'-GATTCCAACTTCATTACTCTG-3') and re-

verse primer R2 (5'-GGTCCATATCTGCCCACTG-3'). β -actin was amplified as a control. As shown in Figure 1D, the specific Gpr128 fragment from WT mice was amplified with forward primer R3 (5'-AACCA-CAAACITTT TCCAATCAA-3') and reverse primer R4 (5'-CCACT CAGGGCATAAATAC TCC-3').

Northern blotting analysis

Total RNA was extracted from adult mouse tissues using Trizol reagent (Invitrogen, Carlsbad, CA, United States) according to the manufacturer's instructions. Northern blotting was performed as described in the manual provided by the manufacturer (Northern Max-Gly; Ambion Inc., Carlsbad, CA, United States). A 1- μ g aliquot was removed from each mRNA sample from adult WT mice for analysis. The probe used for *Gpr128* was a 715-bp DNA fragment prepared from mouse intestine cDNA using the PCR forward primer N1 (5'-AGAGTCGA-CAGACAGACCACTGAAGGGAAG-3') and reverse primer N2 (5'-TGGCA TCAAAATCTGACTC-3'). Probe DNA (25 ng) was labeled with [³²P]-dATP using a Random Primer Labeling Kit (NEBlot Kit, NEB, Beverly, MA, United States) and subsequently purified by gel filtration.

Maintenance and body weight studies of Gpr128-deficient mice

All mice used in this study were on a mixed 129/BL6 background. The mouse colony was maintained in a temperature- and humidity-controlled room with a 12:12-h light-dark cycle, and the mice were fed a standard laboratory chow diet with free access to water. The animals were maintained by crossing heterozygous progeny.

Beginning at the age of 4 wk, body weights were recorded every 4 wk. Animals of both sexes were used, but littermates were matched by gender.

Histology and immunofluorescence staining

The intestines of WT and *Gpr128*^{-/-} mice at 8 wk of age were collected and fixed with 10% formalin for sectioning followed by hematoxylin and eosin (HE) staining. Sections (6 mm) were cut and stained with HE according to standard procedures. For immunofluorescence analysis, paraffin-embedded sections were deparaffinized with xylene and treated with gradually decreasing concentrations of ethanol. The sections were blocked for 1 h in 5% bovine serum followed by staining overnight at 37 °C with goat anti-GPR128 antibodies (sc-48208, Santa-Cruz Biotechnology Inc., Santa-Cruz, CA, United States) for human and mouse tissues and finally incubated with fluorescent-conjugated secondary antibody for 30 min. Finally, the slides were rinsed with PBS and mounted with VECTASHIELD mounting medium (H-1200, Vector Laboratories Inc., Burlingame, CA, United States).

Food consumption studies and fecal quantity analysis

At week 16 of the experimental diet period, the mice were

individually caged and given preweighed food for 5 d. During this period, the amount of food consumed was determined, and feces were quantitatively collected over a 24 h period. The results are expressed as grams of food consumed and feces excreted per day.

Analyses for the constituents of the blood and plasma

After the 32 wk experimental feeding period, the mice were fasted for 16 h and subsequently anesthetized with ketamine and xylazine diluted in 0.9% saline. Blood was removed by cardiac puncture into tubes containing 1 mmol/L EDTA. White adipose (epididymal and uterine fat pads) and brown adipose (intrascapular) tissue as well as the heart, liver, spleen, lungs, and kidneys were removed, and the wet weight of each was recorded.

Blood samples were collected for complete blood counts including white blood cells, red blood cells, hemoglobin, hematocrit, mean corpuscular volume, mean corpuscular hemoglobin, mean corpuscular hemoglobin concentration, platelets, white-small cell rate, white-middle cell rate, and white-large cell rate using an automated hematology analyzer (Poch-100ivd, Sysmex, Kobe, Japan). Plasma was obtained by low-speed centrifugation of the blood samples for measurement of albumin/globulin, globulin, low-density lipoprotein cholesterol, albumin, alkaline phosphatase, alanine aminotransferase, aspartate aminotransferase, urea nitrogen, creatinine, glucose, high-density lipoprotein cholesterol, lactate dehydrogenase, total cholesterol, triglycerides and total protein using an automated chemistry analyzer (CHEMIX-180; Sysmex, Kobe, Japan).

Analysis of intestine motility

Male and female mice at 8 and 32 wk of age were sacrificed. A Trendelenburg preparation was utilized to examine intestinal motility in WT and *Gpr128*^{-/-} mice. Briefly, the jejunum was removed and placed in pre-oxygenated Krebs's Ringer solution at room temperature. A segment of the jejunum (6 cm long) was placed into an organ bath and was superfused with oxygenated Krebs solution at 37 °C. Both ends of the jejunum were catheterized. The proximal tube was connected to a syringe cylinder (for altering the resting intraluminal pressure) and a pressure transducer *via* a three-way stopcock. A glass micropipette (tip diameter approximately 50 μm) was placed on the intestinal wall to record the slow waves through gentle suction. The peristalsis and slow waves were fed into a computer through the Micro1401 interface (Cambridge Electronic Design, United Kingdom) and analyzed using the Spike2 program (CED, United Kingdom). The preparation was allowed to stabilize for at least 40 min before the experiments were started.

Statistical analysis

The data are presented as the mean ± SD. Differences between groups were determined by the 2-tailed Student *t* test. *P* values less than 0.05 were considered significant.

RESULTS

Targeted disruption of the *Gpr128* gene

To investigate the potential roles of *Gpr128* in mice, we generated a targeted disruption of the mouse *Gpr128* gene in ES cells by homologous recombination. In the targeting vector, 3 exons (10, 11 and 12), which encode the GPS domain and a portion of 7TM domain, were replaced with a PGK cassette followed by the neomycin resistance gene (Figure 1A). After electroporating ES cells with the linearized targeting vector under positive-negative selection, we identified three targeted ES clones by PCR (Figure 1B). Two of these clones were microinjected into C57BL/6 blastocysts to obtain chimeras. Mice heterozygous for *Gpr128* showed normal development and were fertile, indicating that the targeted locus does not have detrimental dominant activity.

The genotypes of the offspring were analyzed by PCR to identify WT (+/+), heterozygous (+/-), and homozygous (-/-) mice. Amplification of the WT and targeted alleles produced bands of 5.4 and 5.7 kb, respectively (Figure 1C). As expected, the ratio of phenotypes was in accord with Mendelian frequency, indicating that there was no increased embryonic mortality in the mutant animals. Semi-quantitative RT-PCR and immunofluorescence staining demonstrated that *Gpr128* was not detected in the intestine of homozygous mice (Figure 1D and E), indicating that we have successfully established a *Gpr128* disruption mouse model.

***Gpr128* is specifically expressed in the mouse intestine**

We investigated the expression pattern of the WT *Gpr128* gene in adult mouse tissues by semi-quantitative RT-PCR, Northern blotting and immunofluorescence staining. *Gpr128* mRNA was highly and exclusively detected in the intestine (Figure 2A, B and D). RT-PCR was then performed to determine the presence of *Gpr128* mRNA throughout the digestive tract and at different postnatal development stages. *Gpr128* expression was detected prominently in the small intestine and colon from postnatal day 0 through 8 wk (Figure 2C). The distribution of Gpr128 protein in the mouse intestine was then analyzed by immunofluorescence staining. We found that the Gpr128 protein was confined to the mucosa. As shown in Figure 2D, Gpr128 expression was restricted to epithelial cells.

***Gpr128*^{-/-} mice gained significantly less body weight than their WT counterparts**

Mice lacking the *Gpr128* gene (*Gpr128*^{-/-}) grew normally and displayed normal reproductive functions on a standard mouse chow diet. We found no differences between *Gpr128*^{+/+} and *Gpr128*^{-/-} mice with respect to food intake or fecal excretion (Figure 3B and C). However, *Gpr128*^{-/-} mice gained less weight on average than their *Gpr128*^{+/+} littermates by 24 wk of age. The body weights of WT and *Gpr128*^{-/-} mice were 30.81 ± 2.84 and 25.74 ± 4.50 g, respectively (Figure 3A, *n* = 10, *P* < 0.01). When separated by sex, both male and female *Gpr128*^{-/-} mice gained

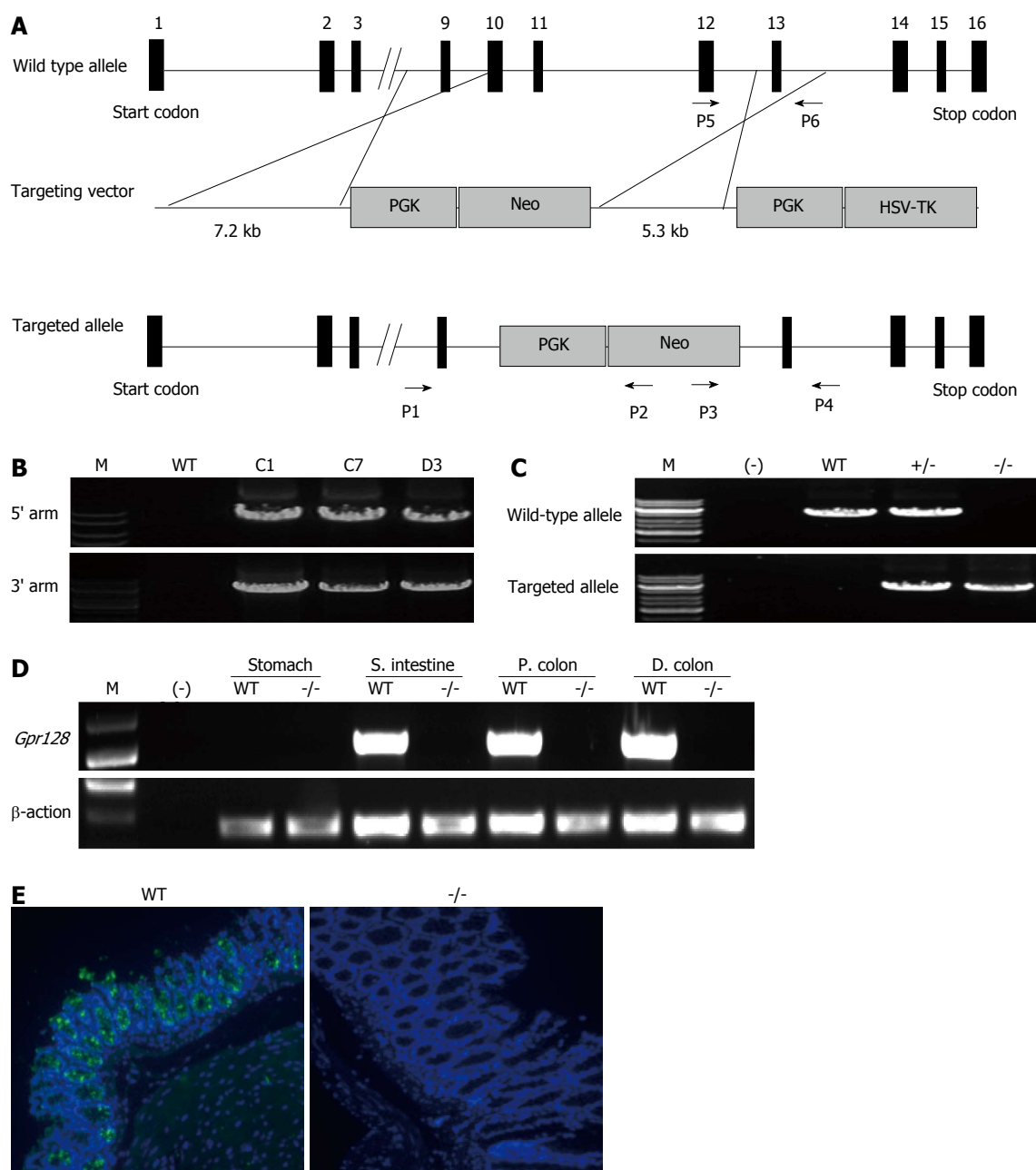


Figure 1 Targeted deletion of *Gpr128* in mice. A: Gene targeting strategy. Numbered boxes represent *Gpr128* coding exons. The start codon and stop codon are indicated as a star and pound sign, respectively. The targeting vector contains a 7.1-kb 5' arm and a 5.3-kb 3' arm. Exons 10, 11 and 12 of the *Gpr128* gene were replaced by a PGK-Neo cassette through homologous recombination. The primer pairs for polymerase chain reaction (PCR) genotyping are indicated by arrows (5' arm: P1, P2; 3' arm: P3, P4); B: PCR screening for targeted embryonic stem (ES) cell clones. Correctly recombined clones show 7.7 and 5.7 kb bands, respectively. Three recombined ES cell clones show the expected bands as detected with primers P1-P4; C: PCR analysis of genomic tail DNA derived from *Gpr128*^{+/+} mouse intercrossing. A 5.4-kb fragment amplified with primers P5 and P6 represents the wild-type (WT) allele. A 5.7-kb band was amplified from the targeted allele with P3 and P4; D: *Gpr128* expression in gastrointestinal tissue with two different genotypes by semiquantitative reverse transcription-polymerase chain reaction. A specific *Gpr128* fragment, which exists in WT mice, was deleted in *Gpr128*^{-/-} mice. The transcript for β -actin was examined as a control for RNA loading and integrity; E: Expression pattern of *Gpr128* protein in WT and *Gpr128*^{-/-} adult mouse colon revealed by immunofluorescence (original magnification, $\times 200$). M: Marker lane; (-): Negative control without template; S. intestine: Small intestine; P. colon: Proximal colon; D. colon: Distal colon.

less weight than their WT counterparts (data not shown). The decreased weight gain in *Gpr128*^{-/-} mice persisted at 28 and 32 wk (26.69 ± 4.29 and 28.46 ± 4.42 g *vs* 33.15 ± 3.20 and 36.75 ± 4.18 g in *Gpr128*^{+/+} mice, $n = 10$, $P < 0.01$, Figure 3A).

To account for the differences in body weight gain between the *Gpr128*^{+/+} and *Gpr128*^{-/-} mice, various tis-

sues were removed and weighed. There were no differences in the epididymal and uterine fat pads, brown fat, or liver weights between male and female *Gpr128*^{+/+} and *Gpr128*^{-/-} mice (Figure 3D). There were also no differences in heart, spleen, lung, and kidney weights between the *Gpr128*^{+/+} and *Gpr128*^{-/-} mice (Figure 3D).

The cell counts and biochemical parameters of the

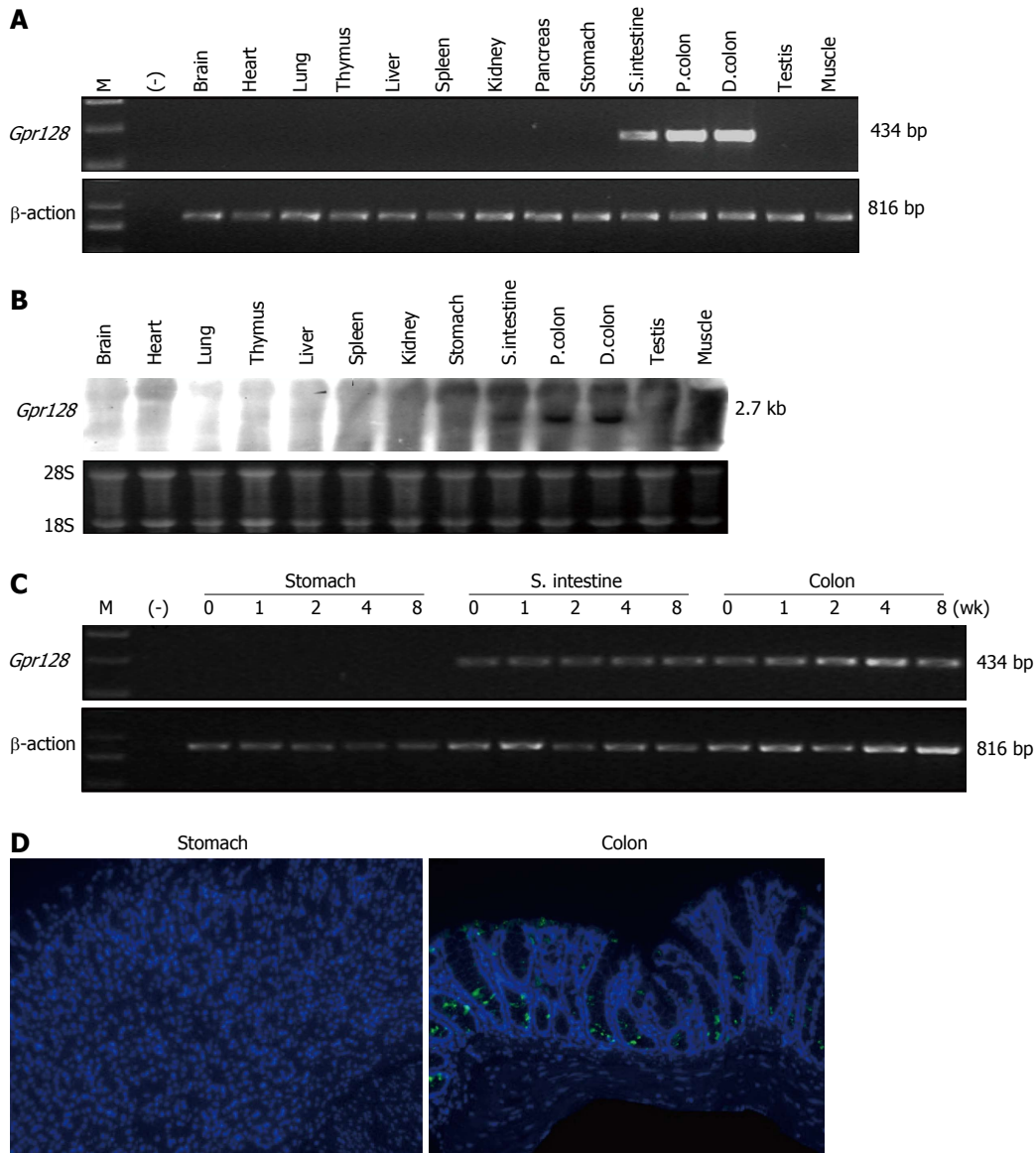


Figure 2 Selective expression of *Gpr128* within the intestine in mice. A: Expression levels of *Gpr128* mRNA. The mRNA levels were examined in major tissues of normal mice using semi-quantitative reverse transcription-polymerase chain reaction (RT-PCR), and the expression level of β -actin was used as an endogenous control. M: Marker lane; (-): Negative control without template; B: Northern blotting analysis of *Gpr128*. Total RNA from wild type mice was extracted and subjected to Northern blotting analysis using a 715-bp fragment of *Gpr128* cDNA corresponding to exons 1 through 6. The bottom lane shows the 28S and 18S ribosomal RNA as a control; C: Examination of the stage-specific expression of *Gpr128* mRNA. RT-PCR was performed throughout the digestive tract and at various postnatal developmental stages to determine the presence of *Gpr128* mRNA from postnatal day 0 through 8 wk; D: Expression pattern of *Gpr128* protein in the stomach and colon of adult WT mouse revealed by immunofluorescence (original magnification, $\times 200$).

blood of *Gpr128*^{-/-} mice were not different from those of the WT mice (Figure 3E and F). Furthermore, there were no overt differences in the gross morphology or histology (HE staining) of the GI tract between the *Gpr128*^{-/-} and the WT mice (data not shown).

Increased frequency of peristalsis and slow waves of the small intestine in *Gpr128*^{-/-} mice

Using a Trendelenburg model, we analyzed the peristalsis and the slow waves of the small intestine (jejunum) in WT and *Gpr128*^{-/-} mice (Figure 4A). The amplitudes of peristaltic movement at resting intraluminal pressures of 0, 1, 2 and 3 cmH₂O were not different between WT and *Gpr128*^{-/-} mice (data not shown). The frequency of peri-

staltic contraction was increased in *Gpr128*^{-/-} mice since 8 wk when the resting intraluminal pressure increased. The frequency of peristalsis was higher in *Gpr128*^{-/-} mice than in WT mice when the resting intraluminal pressure was 3 cmH₂O (6.6 ± 2.3 peristalsis/15 min in *Gpr128*^{-/-} intestine *vs* 2.6 ± 1.7 peristalsis/15 min in WT intestine, $n = 5$, $P < 0.05$, Figure 4B). At the age of 32 wk, the frequency of peristalsis was higher in *Gpr128*^{-/-} mice than in WT mice when the resting intraluminal pressure was 2 or 3 cmH₂O (8.3 ± 3.0 and 7.4 ± 3.1 peristalsis/15 min in *Gpr128*^{-/-} intestine *vs* 4.6 ± 2.3 and 3.1 ± 0.8 peristalsis/15 min in WT intestine, $n = 8$, 2 cmH₂O: $P < 0.05$, 3 cmH₂O: $P < 0.01$, Figure 4C) and the frequency of slow waves was also higher in *Gpr128*^{-/-} intestine compared

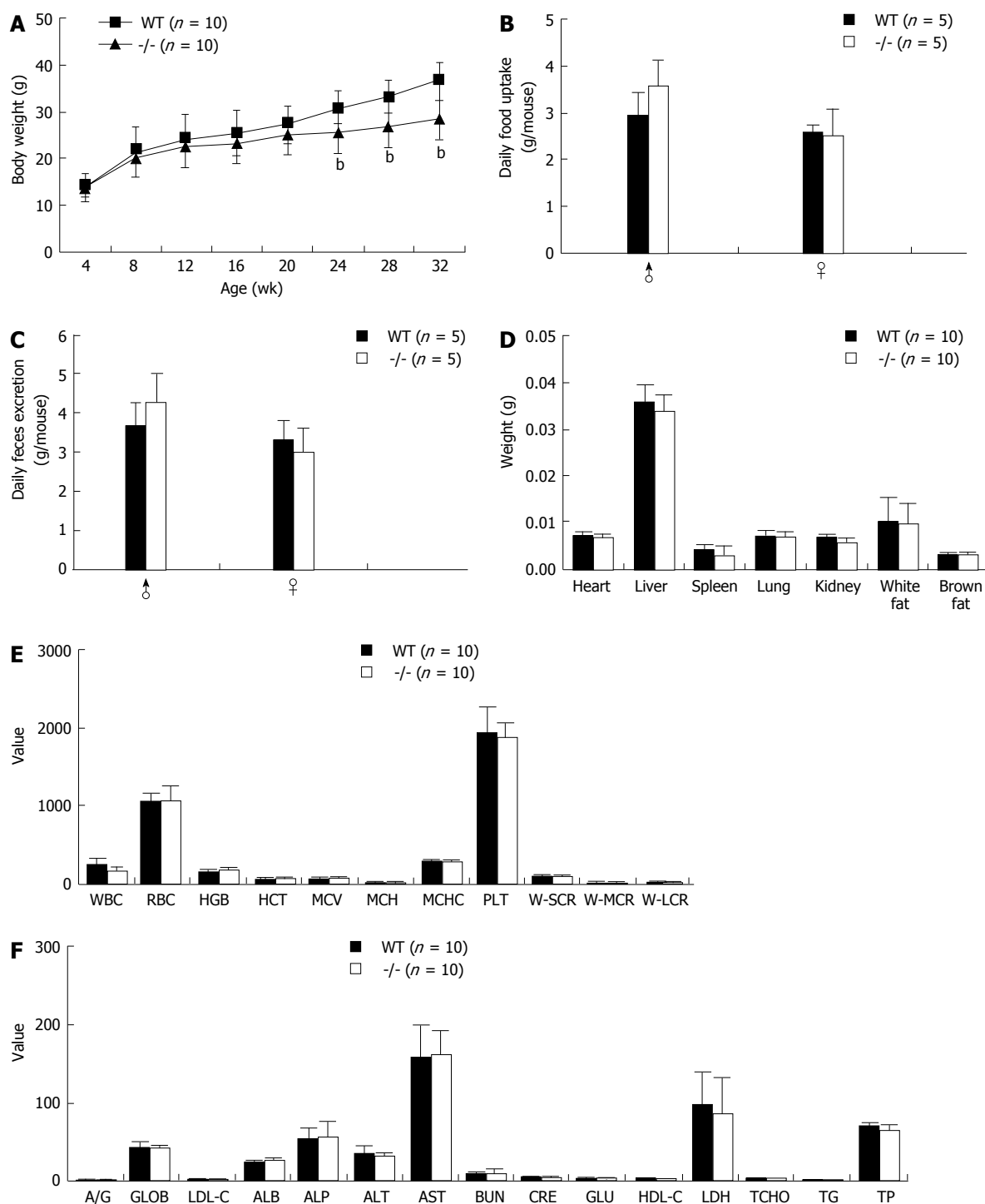


Figure 3 Deletion of *Gpr128* results in reduced body weight gain in mice. A: An analysis of the body weight of mice of different genotypes shows that *Gpr128*^{-/-} mice have a reduced body weight (*P* values of weeks 24, 28 and 32 are 0.0065, 0.0010 and 0.0003); B: Daily food intake of 16-wk-old mice of different genotypes (*P* > 0.05); C: Daily fecal excretion of 16-wk-old mice of different genotypes (*P* > 0.05); D: Organs isolated from 32-wk-old animals weighed and correlated to body weight (*P* > 0.05); E: Blood routine test of 32-wk-old animals using an automated hematology analyzer (*P* > 0.05; WBC: White blood cells; RBC: Red blood cells; HGB: Hemoglobin; HCT: Hematocrit; MCV: Mean corpuscular volume; MCH: Mean corpuscular hemoglobin; MCHC: Mean corpuscular hemoglobin concentration; PLT: Platelet; W-SCR: White-small cell rate; W-MCR: White-middle cell rate; W-LCR: White-large cell rate); F: Biochemical parameters of 32-wk-old animals using an automated chemistry analyzer (*P* > 0.05; A/G: Albumin/globulin; GLOB: Globulin; LDL-C: Low-density lipoprotein cholesterol; ALB: albumin; ALP: alkaline phosphatase; ALT: Alanine aminotransferase; AST: Aspartate aminotransferase; BUN: Urea nitrogen; CRE: Creatinine; GLU: Glucose; HDL-C: High-density lipoprotein cholesterol; LDH: Lactate dehydrogenase; TCHO: Total cholesterol; TG: Triglyceride; TP: Total protein). All values are mean ± SD (*n* = 10, ^b*P* < 0.01 vs wild-type group).

with WT intestine (30.6 ± 4.2 , 31.4 ± 3.9 , and 31.9 ± 4.5 /min and 35.8 ± 4.3 , 36.4 ± 4.2 , and 37.1 ± 4.8 /min in normal and *Gpr128*^{-/-} mice, respectively, *n* = 8, *P* < 0.05, Figure 4D).

DISCUSSION

Here, we describe the first genetic analysis of *Gpr128* function in a mammalian model. A targeted mutation of

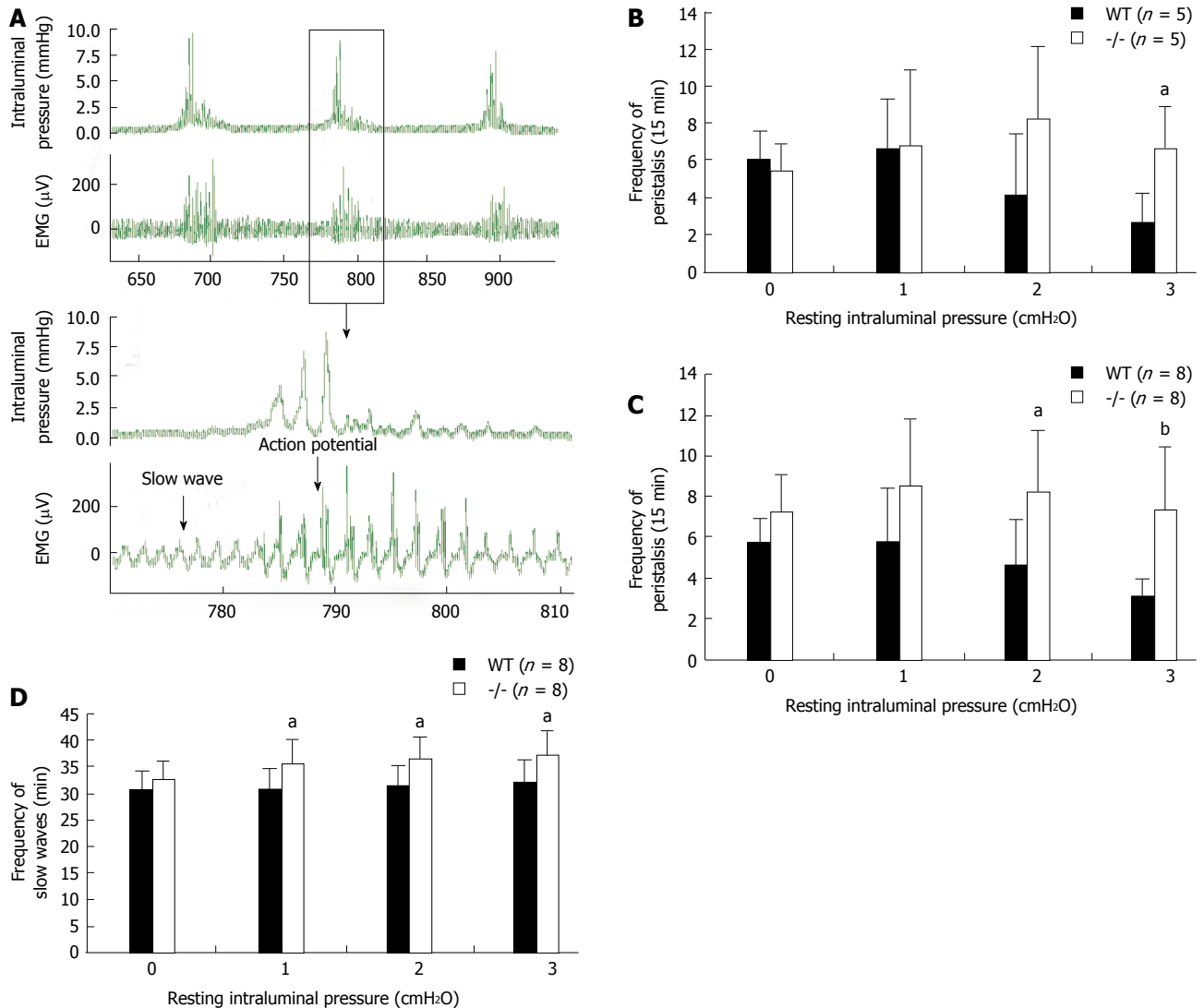


Figure 4 *Gpr128* deficiency leads to increased frequency of intestinal contraction. **A:** The raw traces of intraluminal pressure of a jejunum segment of *Gpr128*^{-/-} mice and the simultaneously recorded extracellular electrical potential from the gut wall. The lower panel of **A** shows an expanded view of the recording within the square of the upper panel; **B:** Frequency of peristalsis in wild-type (WT) and *Gpr128*^{-/-} mice of 8 wk. The frequency of peristalsis was increased in *Gpr128*^{-/-} mice at a resting intraluminal pressure of 3 cmH₂O ($n = 5$, $P = 0.0137$); **C:** Frequency of peristalsis in WT and *Gpr128*^{-/-} mice of 32 wk. The frequency of peristalsis was increased in *Gpr128*^{-/-} mice at resting intraluminal pressures of 2 and 3 cmH₂O ($n = 8$, 2 cmH₂O: $P = 0.0166$, 3 cmH₂O: $P = 0.0020$); **D:** Frequency of slow waves in WT and *Gpr128*^{-/-} mice of 32 wk. The frequency of slow waves was increased in *Gpr128*^{-/-} mice at resting intraluminal pressures of 1, 2 and 3 cmH₂O ($n = 8$, 1 cmH₂O: $P = 0.0303$, 2 cmH₂O: $P = 0.0271$, and 3 cmH₂O: $P = 0.0402$). All values are mean \pm SD (^a $P < 0.05$, ^b $P < 0.01$ vs wild-type group).

GPR128 causes a deletion of part of the 7TM region (Figure 1A) and is presumably a null allele. Residual WT transcripts could not be detected in the intestines of mutant mice (Figure 1D and E).

GPR128 is an orphan GPCR, the physiological function of which is unknown. To explore the role of *Gpr128*, we first examined its expression profile in different tissues. We found that *Gpr128* mRNA expression is exclusively confined to the small intestine and colon. Through immunofluorescence staining, *Gpr128* immunoreactivity was detected in the mucosa of the intestine and was found to be restricted to epithelial cells.

The cell count and biochemical parameters of *Gpr128*^{-/-} mice were not different from those of their WT counterparts, indicating that *Gpr128* is not essential for the maintenance of homeostasis.

A major finding in the *Gpr128*^{-/-} mice was the lower body weight gain compared with the WT littermates by 24 wk of age when the animals were maintained on a standard laboratory rodent chow diet. Additionally, there were no significant differences in the weights of epididymal or uterine fat pads, brown fat, or the liver between WT and *Gpr128*^{-/-} mice. These data suggest that the observed weight difference between the mice was not due to reduced adiposity in the *Gpr128* knockout mice.

A number of factors may potentially participate in the regulation of energy balance and weight gain, including gastric emptying^[25], gastrointestinal motility^[26] as well as gastrointestinal peptides such as ghrelin and cholecystokinin. The release of these two hormones is known to be regulated by ingestion and their action may in turn regulate gastrointestinal function and food intake^[29,30].

However, given that *Gpr128*^{-/-} and WT mice consumed equivalent amounts of chow, the excretion of feces was similar in the two groups and *Gpr128* was confined to the intestinal tissue, we tested the potential differences in intestinal motility between *Gpr128*^{-/-} and WT mice. The frequency of peristaltic movement and slow waves were found to be increased in *Gpr128*^{-/-} intestine compared with WT intestine. Despite similar levels of chow consumption, *Gpr128*^{-/-} mice colonized with the model fermentative community are significantly leaner and lighter than their WT littermates because their increased intestinal motility reduces the time required to harvest energy from the diet^[31]. Whether the increase in gut motility accounts for the lower weight gain in *Gpr128*^{-/-} mice awaits further investigation. Because peristalsis is known to be regulated by the enteric nerve plexus^[32], whereas the slow waves are known to originate from the interstitial cells of Cajal^[33], further studies should be conducted to examine their development and function in *Gpr128*^{-/-} mice. Given the epithelial localization of Gpr128 within the gut, it will also be important to explore its role in the regulation of intestinal secretion and absorption.

In summary, the present study shows that *Gpr128* is expressed exclusively in the small and large intestine, and *Gpr128* deficiency resulted in a decrease in body weight gain and an increase in intestinal motility. The potential for *Gpr128* as a novel therapeutic target for obesity and nutritional disorders is worth exploring.

COMMENTS

Background

The Adhesion family is the second largest subfamily of G-protein-coupled receptors (GPCR) which is one of the largest superfamilies of cell-surface receptors. Family members are characterized by the dual presence of a secretin-like seven-transmembrane domain and a long cell adhesion-like N-terminus that typically contains one functional GPCR proteolytic site domain domain; however, the function of most of these receptors is still not understood.

Research frontiers

An orphan receptor of the Adhesion-GPCR *GPR128* was identified during BLASTP searches of the Celera database in 2003. The tissue distribution of *GPR128* derived from the EST data shows specific pattern in humans and mice. The physiological function of *GPR128* in mammals is still unknown.

Innovations and breakthroughs

In this study, the authors generated a targeted deletion of *Gpr128* mouse model to explore the biological function of *Gpr128*. Furthermore, they found that *Gpr128* is exclusively expressed in mouse intestinal tissue. Finally, we showed that the targeted deletion of the orphan adhesion-GPCR *Gpr128* resulted in reduced body weight gain and increased intestinal contraction frequency in mice.

Applications

The present findings regarding the activities of *Gpr128* in mouse intestinal cells showed for the first time that *Gpr128* is a regulator of host energy balance and may help explain the biological functions of *Gpr128* in the intestine. Future studies are needed to identify the ligands of *Gpr128* which are often the key to determining the functional role, and to determine the mechanism by which *Gpr128* regulates intestinal contraction frequency. *Gpr128* may be a potential drug target and may be useful for the development of novel therapies for obesity and nutritional disorders.

Terminology

GPCRs constitute one of the largest protein families in humans. GPCRs receive extracellular signals and transmit them into cells via an intracellular signaling pathway that employs different G-proteins. The GPCR family has attracted significant attention from researchers due to its important role in drug discovery.

Peer review

After the generation of a *Gpr128* gene knockout mouse model and the investigation of its phenotypes and the biological function of *Gpr128*, the authors found that the deletion of *Gpr128* in mice resulted in weight loss and increased intestinal contraction frequency. The authors attempted to demonstrate the relationship between weight loss and intestinal motility. Overall, this study fits nicely within the scope of the journal. The data are generally clean and could potentially uncover the physiological roles of *Gpr128*, which is of value to the field.

REFERENCES

- 1 **Lander ES**, Linton LM, Birren B, Nusbaum C, Zody MC, Baldwin J, Devon K, Dewar K, Doyle M, FitzHugh W, Funke R, Gage D, Harris K, Heaford A, Howland J, Kann L, Lehoczký J, LeVine R, McEwan P, McKernan K, Meldrim J, Mesirov JP, Miranda C, Morris W, Naylor J, Raymond C, Rosetti M, Santos R, Sheridan A, Sougnez C, Stange-Thomann N, Stojanovic N, Subramanian A, Wyman D, Rogers J, Sulston J, Ainscough R, Beck S, Bentley D, Burton J, Clee C, Carter N, Coulson A, Deadman R, Deloukas P, Dunham A, Dunham I, Durbin R, French L, Grafham D, Gregory S, Hubbard T, Humphray S, Hunt A, Jones M, Lloyd C, McMurray A, Matthews L, Mercer S, Milne S, Mullikin JC, Mungall A, Plumb R, Ross M, Showkneen R, Sims S, Waterston RH, Wilson RK, Hillier LW, McPherson JD, Marra MA, Mardis ER, Fulton LA, Chinwalla AT, Pepin KH, Gish WR, Chissole SL, Wendl MC, Delehaunty KD, Miner TL, Delehaunty A, Kramer JB, Cook LL, Fulton RS, Johnson DL, Minx PJ, Clifton SW, Hawkins T, Branscomb E, Predki P, Richardson P, Wenning S, Slezak T, Doggett N, Cheng JF, Olsen A, Lucas S, Elkin C, Uberbacher E, Frazier M, Gibbs RA, Muzny DM, Scherer SE, Bouck JB, Sodergren EJ, Worley KC, Rives CM, Gorrell JH, Metzker ML, Naylor SL, Kucherlapati RS, Nelson DL, Weinstock GM, Sakaki Y, Fujiiyama A, Hattori M, Yada T, Toyoda A, Itoh T, Kawagoe C, Watanabe H, Totoki Y, Taylor T, Weissenbach J, Heilig R, Saurin W, Artiguenave F, Brottier P, Bruls T, Pelletier E, Robert C, Wincker P, Smith DR, Doucette-Stamm L, Rubenfield M, Weinstock K, Lee HM, Dubois J, Rosenthal A, Platzer M, Nyakatura G, Taudien S, Rump A, Yang H, Yu J, Wang J, Huang G, Gu J, Hood L, Rowen L, Madan A, Qin S, Davis RW, Federspiel NA, Abola AP, Proctor MJ, Myers RM, Schmutz J, Dickson M, Grimwood J, Cox DR, Olson MV, Kaul R, Raymond C, Shimizu N, Kawasaki K, Minoshima S, Evans GA, Athanasiou M, Schultz R, Roe BA, Chen F, Pan H, Ramser J, Lehrach H, Reinhardt R, McCombie WR, de la Bastide M, Dedhia N, Blöcker H, Hornischer K, Nordsiek G, Agarwala R, Aravind L, Bailey JA, Bateman A, Batzoglou S, Birney E, Bork P, Brown DG, Burge CB, Cerutti L, Chen HC, Church D, Clamp M, Copley RR, Doerks T, Eddy SR, Eichler EE, Furey TS, Galagan J, Gilbert JG, Harmon C, Hayashizaki Y, Haussler D, Hermjakob H, Hokamp K, Jang W, Johnson LS, Jones TA, Kasif S, Kasprzyk A, Kennedy S, Kent WJ, Kitts P, Koonin EV, Korf I, Kulp D, Lancet D, Lowe TM, McLysaght A, Mikkelsen T, Moran JV, Mulder N, Pollara VJ, Ponting CP, Schuler G, Schultz J, Slater G, Smit AF, Stupka E, Szustakowski J, Thierry-Mieg D, Thierry-Mieg J, Wagner L, Wallis J, Wheeler R, Williams A, Wolf YI, Wolfe KH, Yang SP, Yeh RF, Collins F, Guyer MS, Peterson J, Felsenfeld A, Wetterstrand KA, Patrino A, Morgan MJ, de Jong P, Catanese JJ, Osogawa K, Shizuya H, Choi S, Chen YJ. Initial sequencing and analysis of the human genome. *Nature* 2001; **409**: 860-921 [PMID: 11237011 DOI: 10.1038/35057062]
- 2 **Venter JC**, Adams MD, Myers EW, Li PW, Mural RJ, Sutton GG, Smith HO, Yandell M, Evans CA, Holt RA, Gocayne JD, Amanatides P, Ballew RM, Huson DH, Wortman JR, Zhang Q, Kodira CD, Zheng XH, Chen L, Skupski M, Subramanian G, Thomas PD, Zhang J, Gabor Miklos GL, Nelson C, Broder S, Clark AG, Nadeau J, McKusick VA, Zinder N, Levine AJ,

- Roberts RJ, Simon M, Slayman C, Hunkapiller M, Bolanos R, Delcher A, Dew I, Fasulo D, Flanigan M, Florea L, Halpern A, Hannenhalli S, Kravitz S, Levy S, Mobarry C, Reinert K, Remington K, Abu-Threideh J, Beasley E, Biddick K, Bonazzi V, Brandon R, Cargill M, Chandramouliswaran I, Charlab R, Chaturvedi K, Deng Z, Di Francesco V, Dunn P, Eilbeck K, Evangelista C, Gabrielian AE, Gan W, Ge W, Gong F, Gu Z, Guan P, Heiman TJ, Higgins ME, Ji RR, Ke Z, Ketchum KA, Lai Z, Lei Y, Li Z, Li J, Liang Y, Lin X, Lu F, Merkulov GV, Milshina N, Moore HM, Naik AK, Narayan VA, Neelam B, Nusskern D, Rusch DB, Salzberg S, Shao W, Shue B, Sun J, Wang Z, Wang A, Wang X, Wang J, Wei M, Wides R, Xiao C, Yan C, Yao A, Ye J, Zhan M, Zhang W, Zhang H, Zhao Q, Zheng L, Zhong F, Zhong W, Zhu S, Zhao S, Gilbert D, Baumhueter S, Spier G, Carter C, Cravchik A, Woodage T, Ali F, An H, Awe A, Baldwin D, Baden H, Barnstead M, Barrow I, Beeson K, Busam D, Carver A, Center A, Cheng ML, Curry L, Danaher S, Davenport L, Desilets R, Dietz S, Dodson K, Doup L, Ferriera S, Garg N, Gluecksmann A, Hart B, Haynes J, Haynes C, Heiner C, Hladun S, Hostin D, Houck J, Howland T, Ibegwam C, Johnson J, Kalush F, Kline L, Koduru S, Love A, Mann F, May D, McCawley S, McIntosh T, McMullen I, Moy M, Moy L, Murphy B, Nelson K, Pfannkoch C, Pratts E, Puri V, Qureshi H, Reardon M, Rodriguez R, Rogers YH, Romblad D, Ruhfel B, Scott R, Sitter C, Smallwood M, Stewart E, Strong R, Suh E, Thomas R, Tint NN, Tse S, Vech C, Wang G, Wetter J, Williams S, Williams M, Windsor S, Winn-Deen E, Wolfe K, Zaveri J, Zaveri K, Abril JF, Guigó R, Campbell MJ, Sjölander KV, Karlak B, Kejariwal A, Mi H, Lazareva B, Hatton T, Narechania A, Diemer K, Muruganujan A, Guo N, Sato S, Bafna V, Istrail S, Lippert R, Schwartz R, Walenz B, Yooseph S, Allen D, Basu A, Baxendale J, Blick L, Caminha M, Carnes-Stine J, Caulk P, Chiang YH, Coyne M, Dahlke C, Mays A, Dombroski M, Donnelly M, Ely D, Esparham S, Fosler C, Gire H, Glanowski S, Glasser K, Glodek A, Gorokhov M, Graham K, Gropman B, Harris M, Heil J, Henderson S, Hoover J, Jennings D, Jordan C, Jordan J, Kasha J, Kagan L, Kraft C, Levitsky A, Lewis M, Liu X, Lopez J, Ma D, Majoros W, McDaniel J, Murphy S, Newman M, Nguyen T, Nguyen N, Nodell M, Pan S, Peck J, Peterson M, Rowe W, Sanders R, Scott J, Simpson M, Smith T, Sprague A, Stockwell T, Turner R, Venter E, Wang M, Wen M, Wu D, Wu M, Xia A, Zandieh A, Zhu X. The sequence of the human genome. *Science* 2001; **291**: 1304-1351 [PMID: 11181995 DOI: 10.1126/science.1058040]
- 3 **Alexander SP**, Mathie A, Peters JA. Guide to Receptors and Channels (GRAC), 5th edition. *Br J Pharmacol* 2011; **164** Suppl 1: S1-324 [PMID: 22040146 DOI: 10.1111/j.1476-5381.2011.01649_1.x]
- 4 **Rosenbaum DM**, Rasmussen SG, Kobilka BK. The structure and function of G-protein-coupled receptors. *Nature* 2009; **459**: 356-363 [PMID: 19458711 DOI: 10.1038/nature08144]
- 5 **Latek D**, Modzelewska A, Trzaskowski B, Palczewski K, Filipek S. G protein-coupled receptors--recent advances. *Acta Biochim Pol* 2012; **59**: 515-529 [PMID: 23251911]
- 6 **Drews J**. Drug discovery: a historical perspective. *Science* 2000; **287**: 1960-1964 [PMID: 10720314 DOI: 10.1126/science.287.5460.1960]
- 7 **Bjarnadóttir TK**, Fredriksson R, Schiöth HB. The adhesion GPCRs: a unique family of G protein-coupled receptors with important roles in both central and peripheral tissues. *Cell Mol Life Sci* 2007; **64**: 2104-2119 [PMID: 17502995 DOI: 10.1007/s00018-007-7067-1]
- 8 **Lagerström MC**, Schiöth HB. Structural diversity of G protein-coupled receptors and significance for drug discovery. *Nat Rev Drug Discov* 2008; **7**: 339-357 [PMID: 18382464 DOI: 10.1038/nrd25182008]
- 9 **Foord SM**, Jupe S, Holbrook J. Bioinformatics and type II G-protein-coupled receptors. *Biochem Soc Trans* 2002; **30**: 473-479 [PMID: 12196118 DOI: 10.1042/BST0300473]
- 10 **Huang YS**, Chiang NY, Hu CH, Hsiao CC, Cheng KF, Tsai WP, Yona S, Stacey M, Gordon S, Chang GW, Lin HH. Activation of myeloid cell-specific adhesion class G protein-coupled receptor EMR2 via ligation-induced translocation and interaction of receptor subunits in lipid raft microdomains. *Mol Cell Biol* 2012; **32**: 1408-1420 [PMID: 22310662 DOI: 10.1128/MCB.06557-11]
- 11 **Yona S**, Lin HH, Siu WO, Gordon S, Stacey M. Adhesion-GPCRs: emerging roles for novel receptors. *Trends Biochem Sci* 2008; **33**: 491-500 [PMID: 18789697 DOI: 10.1016/j.tibs.2008.07.005]
- 12 **Davies B**, Baumann C, Kirchhoff C, Ivell R, Nubbemeyer R, Habenicht UF, Theuring F, Gottwald U. Targeted deletion of the epididymal receptor HE6 results in fluid dysregulation and male infertility. *Mol Cell Biol* 2004; **24**: 8642-8648 [PMID: 15367682 DOI: 10.1128/MCB.24.19.8642-8648.2004]
- 13 **Piao X**, Hill RS, Bodell A, Chang BS, Basel-Vanagaite L, Straussberg R, Dobyns WB, Qasrawi B, Winter RM, Innes AM, Voit T, Ross ME, Michaud JL, Descarrie JC, Barkovich AJ, Walsh CA. G protein-coupled receptor-dependent development of human frontal cortex. *Science* 2004; **303**: 2033-2036 [PMID: 15044805 DOI: 10.1126/science.1092780]
- 14 **Luo R**, Jeong SJ, Jin Z, Strokes N, Li S, Piao X. G protein-coupled receptor 56 and collagen III, a receptor-ligand pair, regulates cortical development and lamination. *Proc Natl Acad Sci USA* 2011; **108**: 12925-12930 [PMID: 21768377 DOI: 10.1073/pnas.1104821108]
- 15 **Shashidhar S**, Lorente G, Nagavarapu U, Nelson A, Kuo J, Cummins J, Nikolich K, Urfer R, Foehr ED. GPR56 is a GPCR that is overexpressed in gliomas and functions in tumor cell adhesion. *Oncogene* 2005; **24**: 1673-1682 [PMID: 15674329 DOI: 10.1038/sj.onc.1208395]
- 16 **Ke N**, Sundaram R, Liu G, Chionis J, Fan W, Rogers C, Awad T, Grifman M, Yu D, Wong-Staal F, Li QX. Orphan G protein-coupled receptor GPR56 plays a role in cell transformation and tumorigenesis involving the cell adhesion pathway. *Mol Cancer Ther* 2007; **6**: 1840-1850 [PMID: 17575113 DOI: 10.1158/1535-7163.MCT-07-0066]
- 17 **Fredriksson R**, Gloriam DE, Höglund PJ, Lagerström MC, Schiöth HB. There exist at least 30 human G-protein-coupled receptors with long Ser/Thr-rich N-termini. *Biochem Biophys Res Commun* 2003; **301**: 725-734 [PMID: 12565841 DOI: 10.1016/S0006-291X(03)00026-3]
- 18 **Fredriksson R**, Schiöth HB. The repertoire of G-protein-coupled receptors in fully sequenced genomes. *Mol Pharmacol* 2005; **67**: 1414-1425 [PMID: 15687224 DOI: 10.1124/mol.104.009001]
- 19 **Insel PA**, Snead A, Murray F, Zhang L, Yokouchi H, Katakia T, Kwon O, Dimucci D, Wilderman A. GPCR expression in tissues and cells: are the optimal receptors being used as drug targets? *Br J Pharmacol* 2012; **165**: 1613-1616 [PMID: 21488863 DOI: 10.1111/j.1476-5381.2011.01434.x]
- 20 **Haitina T**, Olsson F, Stephansson O, Alsjö J, Roman E, Ebdendal T, Schiöth HB, Fredriksson R. Expression profile of the entire family of Adhesion G protein-coupled receptors in mouse and rat. *BMC Neurosci* 2008; **9**: 43 [PMID: 18445277 DOI: 10.1186/1471-2202-9-43]
- 21 **Badiali L**, Cedernaes J, Olszewski PK, Nylander O, Vergoni AV, Schiöth HB. Adhesion GPCRs are widely expressed throughout the subsections of the gastrointestinal tract. *BMC Gastroenterol* 2012; **12**: 134 [PMID: 23009096 DOI: 10.1186/1471-230X-12-134]
- 22 **Lee EC**, Yu D, Martinez de Velasco J, Tessarollo L, Swing DA, Court DL, Jenkins NA, Copeland NG. A highly efficient Escherichia coli-based chromosome engineering system adapted for recombinogenic targeting and subcloning of BAC DNA. *Genomics* 2001; **73**: 56-65 [PMID: 11352566 DOI: 10.1006/geno.2000.6451]
- 23 **Liu P**, Jenkins NA, Copeland NG. A highly efficient recombining-based method for generating conditional knockout

- mutations. *Genome Res* 2003; **13**: 476-484 [PMID: 12618378 DOI: 10.1101/gr.749203]
- 24 **Nagy A**, Rossant J, Nagy R, Abramow-Newerly W, Roder JC. Derivation of completely cell culture-derived mice from early-passage embryonic stem cells. *Proc Natl Acad Sci USA* 1993; **90**: 8424-8428 [PMID: 8378314 DOI: 10.1073/pnas.90.18.8424]
- 25 **Cunningham KM**, Daly J, Horowitz M, Read NW. Gastrointestinal adaptation to diets of differing fat composition in human volunteers. *Gut* 1991; **32**: 483-486 [PMID: 2040469 DOI: 10.1136/gut.32.5.483]
- 26 **Boyd KA**, O'Donovan DG, Doran S, Wishart J, Chapman IM, Horowitz M, Feinle C. High-fat diet effects on gut motility, hormone, and appetite responses to duodenal lipid in healthy men. *Am J Physiol Gastrointest Liver Physiol* 2003; **284**: G188-G196 [PMID: 12409281 DOI: 10.1152/ajpgi.00375.2002]
- 27 **Lee HM**, Wang G, Englander EW, Kojima M, Greeley GH. Ghrelin, a new gastrointestinal endocrine peptide that stimulates insulin secretion: enteric distribution, ontogeny, influence of endocrine, and dietary manipulations. *Endocrinology* 2002; **143**: 185-190 [PMID: 11751608 DOI: 10.1210/en.143.1.185]
- 28 **Verhulst PJ**, Depoortere I. Ghrelin's second life: from appetite stimulator to glucose regulator. *World J Gastroenterol* 2012; **18**: 3183-3195 [PMID: 22783041]
- 29 **French SJ**, Murray B, Rumsey RD, Fadzlin R, Read NW. Adaptation to high-fat diets: effects on eating behaviour and plasma cholecystokinin. *Br J Nutr* 1995; **73**: 179-189 [PMID: 7718539 DOI: 10.1079/BJN19950022]
- 30 **Stengel A**, Taché Y. Interaction between gastric and upper small intestinal hormones in the regulation of hunger and satiety: ghrelin and cholecystokinin take the central stage. *Curr Protein Pept Sci* 2011; **12**: 293-304 [PMID: 21428875 DOI: 10.2174/138920311795906673]
- 31 **Samuel BS**, Shaito A, Motoike T, Rey FE, Backhed F, Manchester JK, Hammer RE, Williams SC, Crowley J, Yanagisawa M, Gordon JI. Effects of the gut microbiota on host adiposity are modulated by the short-chain fatty-acid binding G protein-coupled receptor, Gpr41. *Proc Natl Acad Sci USA* 2008; **105**: 16767-16772 [PMID: 18931303 DOI: 10.1073/pnas.0808567105]
- 32 **Costa M**, Brookes SJ, Hennig GW. Anatomy and physiology of the enteric nervous system. *Gut* 2000; **47** Suppl 4: iv15-iv19; discussion iv26 [PMID: 11076898 DOI: 10.1136/gut.47.suppl_4.iv15]
- 33 **Huizinga JD**, Zarate N, Farrugia G. Physiology, injury, and recovery of interstitial cells of Cajal: basic and clinical science. *Gastroenterology* 2009; **137**: 1548-1556 [PMID: 19778538 DOI: 10.1053/j.gastro.2009.09.023]

P- Reviewers: Han JY, Nakajima N, Tu Y **S- Editor:** Gou SX
L- Editor: Wang TQ **E- Editor:** Wang CH





百世登

Baishideng®

Published by **Baishideng Publishing Group Co., Limited**

Flat C, 23/F., Lucky Plaza,

315-321 Lockhart Road, Wan Chai, Hong Kong, China

Fax: +852-65557188

Telephone: +852-31779906

E-mail: bpgoffice@wjgnet.com

<http://www.wjgnet.com>



ISSN 1007-9327



9 771007 932045